RESEARCH PAPER

Nano-Structured Lipid Carrier for Intestinal Permeation Enhancement of Linagliptin

Saad M. Thamer *, Mohammed S. Al-lami *

Department of Pharmaceutics, College of Pharmacy, University of Basrah, Basrah, Iraq

ARTICLE INFO

Article History:

Received 18 September 2025 Accepted 13 November 2025 Published 01 January 2026

Keywords:

Ex-vivo intestinal permeation Linagliptin NLCs Oral bioavailability P-glycoprotein inhibition

ABSTRACT

Linagliptin, a novel anti-diabetic drug, is a DPP-4 inhibitor used in the treatment of type II diabetes. One of the major disadvantages of Linagliptin is its low oral bioavailability of 29.5% due to first-pass metabolism and P-gp efflux. In an attempt to increase the oral bioavailability, Linagliptin nanostructured lipid carrier were developed with Glyceryl monostearate, Oleic acid and Tween 80 as P-gp inhibitors. Linagliptin nanostructured lipid carrier were formulated using Glyceryl monostearate, Oleic acid, Tween 80 and PEG-400 as solid lipid, oil, surfactant and co surfactant, respectively. Twenty-seven formulations were prepared by the hot emulsification-ultrasonication technique. Particle size, poly dispersity index, entrapment efficiency were evaluated as responses. An optimized formula was evaluated for intestinal transport of Linagliptin by the exvivo intestinal permeation study using the non-everted sac model of Male Sprague Dawley rats. The mean particle size, polydispersity index, entrapment efficiency and zeta potential of the optimized formula were found to be 46.13 \pm 2.19 nm, 0.279 \pm 0.026, 79.75 \pm 0.87% and – 12.8 \pm 4.3 My respectively. The permeation study showed of 2.97 and 2.98 times increment in the in the flux and permeability coefficient in comparison to Linagliptin suspension. The enhanced linagliptin permeation may be due to P-gp efflux inhibition and lymphatic targeting. Thus, Linagliptin nanostructured lipid carrier can be considered promising carriers for oral delivery.

How to cite this article

Thamer S., Al-lami M. Al-lami. Nano-Structured Lipid Carrier for Intestinal Permeation Enhancement of Linagliptin. J Nanostruct, 2026; 16(1):239-260. DOI: 10.22052/JNS.2026.01.022

INTRODUCTION

Diabetes mellitus is a chronic metabolic disorder marked by inadequate insulin secretion, diminished insulin efficacy, or a combination of both, resulting in hyperglycemia. Pharmaceutical specialists are continually looking for innovative alternatives for diabetes management [1, 2].

The American Diabetes Association guidelines for diabetes management identify dipeptidylpeptidase (DPP)-4 inhibitors as therapeutic

* Corresponding Author Email: pgs.saad.thamer@uobasrah.edu.iq

options, resulting in their extensive incorporation into clinical practice. DPP-4 inhibitors operate by regulating the levels of various intestinal hormones, such as incretin, active glucagon-like peptide (GLP)-1, and gastric inhibitory peptide (GIP). Their superiority over current therapy is attributed to a diminished risk of weight gain and hypoglycemia [3].

Linagliptin (LGN) is a potent DPP-4 inhibitor that was approved by the US Food and Drug

Administration (FDA) in 2011 for the treatment of type II diabetes mellitus. LGP is a more effective DPP-4 inhibitor than other choices due to its unique pharmacokinetic/pharmacodynamic profile and lack of drug interactions. LGP immediate- and extended-release ts are available alone or in fixed-dose combinations with other oral anti-diabetics. First-pass metabolism, poor penetration, and P-glycoprotein efflux reduce the medication's oral bioavailability to 29.5% [4-6].

A limited number of studies have attempted to address some issues related to the bioavailability of LGP. Patel *et al.* formulated LGP solid SMEDDS using Labrasol, and Transcutol HP, Capmul MCM as the surfactant, co-surfactant and oil respectively, and conducted optimization by D-optimal mixture design [7]. Veni *et al.* developed solid lipid nanoparticles to mitigate first-pass metabolism [8], whereas Shaik et al. used natural polyphenols, including gallic acid and ellagic acid, to inhibit P-glycoprotein and enhance bioavailability [6].

To date, no study group has tried to use lipid nanoparticles in conjunction with a surfactant and oils that exhibit P-glycoprotein inhibitory activity. Nano-structured lipid carriers (NLCs) have garnered significant attention as innovative nanoparticulate drug carriers due to their advantages, including the capacity to incorporate hydrophobic and hydrophilic drugs, targeted drug delivery, elimination of organic solvents, excellent tolerability and stability, and feasibility for largescale production [9]. NLCs delivered via the oral route demonstrate lymphatic drug transport as the primary mode of drug absorption, circumventing first-pass metabolism. Lipid nanoparticles traverse the digestion and absorption phases, thereafter entering the circulatory system to enhance the oral bioavailability of the lipid-encapsulated medication [10].

This study aimed to develop LGN-NLCs using lipids with surfactant characteristics, fatty acids as the oil, and Tween 80 besides span 80 as both a surfactant and a P-gp inhibitor, based on the hypothesis that evading first-pass metabolism through lymphatic transport, combined with P-gp inhibition, could improve oral bioavailability. And according to the particle size, zeta potential, polydispersity index (PDI) and entrapment efficiency, optimized formulation has to find out and examine for the *ex-vivo* intestinal permeation study using the non-everted sac model of albino Wistar rat.

MATERIALS AND METHODS

Materials

LGP was purchased from BID pharmatech-Chemicals Ltd., China. Stearic acid (S.A) and glyceryl behenate (G.B) from BDH Chemicals Ltd. Poole, England. Glyceryl monostearate (GMS) and cetyl alcohol (C.A) from Baoji Guokang Bio-tech. co, Ltd in china. Tween 80 and span 80 purchased from Thomas Baker-India. Oleic acid and olive oil from Loba Chemie Pvt. Ltd., Mumbai, India. PG and all grades of PEG (200, 400 and 600) purchased from Provizer Pharma, India. Dialysis membrane (MWCO: 12–14 K) was purchased from HiMedia Laboratories Pvt. Ltd., Mumbai, India. All other chemicals utilized in the experiment were of analytical reagent grade. Double distilled water was used throughout the experimentation.

Methods

Determination of Solubility in Various Lipids

The most important feature for the selection of the starting materials is the solubility of drug in both solid and liquid different lipids.

Solubility in Solid Lipid

Related to the ability of lipids to solubilize LGN The solubility of LGP in different lipids, including glyceryl monostearate, stearic acid, glyceryl behenate, and cetyl alcohol, was evaluated. A precise amount of LGP (5 mg) was measured and added into 50 mg of molten lipid while stirring with a magnet stirrer. Furthermore, a prescribed amount of fat was gradually added with stirring and heating until a clear solution was obtained. The total amount of each lipid that could have been contained in the complete solubility of LGP was recorded. The experiment was reproduced three times and results were reported as mean value (mg/g) ± standard deviation (SD) [11].

Solubility in Liquid Lipid (Oils)

Oleic acid, castor oil, cottonseed oil, and olive oil were evaluated for LGN solubility. To achieve this, an excess amount of LGN was added to 5mL of each oil in 10mL screw-capped tubes, which were kept in a water bath shaker at a constant stirring for 72 h at 37°C. The supernatant was carefully collected and filtered by 0.45µm membrane filter after centrifugation of the mixture for 15 minutes at 5000 rpm. The filtrate was then appropriately diluted with methanol and measuring the UV absorbance at predetermined maximum

wavelength to determine LGN concentration in different oils. A blank solution was prepared from the corresponding oil diluted in methanol at the same dilution factor as the samples [12].

Preparation of LGP-NLCs

LGN-NLCs were prepared by modified hot emulsification-ultrasonication technique [13]. A binary lipid blend of solid and liquid lipids of those with the highest solubility profiles were combined with 10 mg of LGN and heated to approximately $10 \pm 0.5^{\circ}\text{C}$ above the melting point of solid lipid

to form a homogeneous and transparent oily solution. An oil-in-water (o/w) pre-emulsion was prepared by gradual addition of the liquefied lipid phase into the preheated aqueous phase of Tween 80 as a surfactant and PEG-400 as a co-surfactant in double distilled water with continuous stirring. Then, the hot nanoemulsion was prepared by probe sonication (Biobase, Germany) for 10 min at 300Watts and cycles of 9 s on/off. Afterward, the nanoemulsion was cooled to allow the formations of LGN-NLCs. A 27 formulas were established to assess different factors affecting the properties of

Table 1. LGN-NLCs formulas.

F	Solid lipid GMS (mg)	Oil O.A (mg)	Surfactant type	Surfactant concentration (%w/v)	Co-surfactant type	Co-surfactant concentration (%w/v)
1	270	30	Tween 80	1	PEG-400	1
2	270	30	Tween 80	1.5	PEG-400	1
3	270	30	Tween 80	2	PEG-400	1
4	270	30	Tween 80	2.5	PEG-400	1
5	270	30	Tween 80	1	PEG-400	1.5
6	270	30	Tween 80	1.5	PEG-400	1.5
7	270	30	Tween 80	2	PEG-400	1.5
8	270	30	Tween 80	2.5	PEG-400	1.5
9	270	30	Tween 80	1	PEG-400	2
10	270	30	Tween 80	1.5	PEG-400	2
11	270	30	Tween 80	2	PEG-400	2
12	270	30	Tween 80	2.5	PEG-400	2
13	270	30	Tween 80	1	PEG-400	2.5
14	270	30	Tween 80	1.5	PEG-400	2.5
15	270	30	Tween 80	2	PEG-400	2.5
16	270	30	Tween 80	2.5	PEG-400	2.5
17	270	30	Span 80	1	PEG-400	1.5
18	270	30	Span 80	1.5	PEG-400	1.5
19	270	30	Span 80	2	PEG-400	1.5
20	270	30	Span 80	2.5	PEG-400	1.5
21	270	30	Tween 80	2.5	PEG-600	1.5
22	270	30	Tween 80	2.5	PEG-200	1.5
23	270	30	Tween 80	2.5	PG	1.5
24	240	60	Tween 80	2.5	PEG-400	1.5
25	210	90	Tween 80	2.5	PEG-400	1.5
26	405	45	Tween 80	2.5	PEG-400	1.5
27	540	60	Tween 80	2.5	PEG-400	1.5

LGN-NLCs and to obtained the optimized formula as shown in table 1 [14].

Determination of Particle Size Distribution and polydispersity index

Dynamic light scattering is the most useful and reliable technique for routine determination of particle size and distribution of nanoparticle dispersion. The Zetasizer NanoZS® (Malvern, UK) was used at a scattering angle of a 173° at 25°C. From the analysis, the mean particle size and polydispersity index (PDI) were used to evaluate of LGN-NLCs. The measurements were done in triplicate, and standard deviations were calculated [15].

Determination of Entrapment Efficiency

The entrapment efficiency (EE %) represents the percentage of LGN encapsulated within the NLC, obtained indirectly by measuring the concentration of free LGN in the dispersion medium. The quantity of unentrapped free medication was ascertained utilizing an ultrafiltration approach [16]. In summary, 5 mL of LGN-NLCs solution was introduced into the upper chamber of a centrifuge tube paired with an ultrafilter possessing a molecular weight cut-off of (MWCO) 10 kDa and subjected to centrifugation for 30 minutes at 4000 rpm. The ultrafiltrate containing the unbound medication was diluted with methanol, and the concentration of unentrapped LGN was quantified spectrophotometrically at the predetermined maximum wavelength. The EE% was determined utilizing Eq. 1:

$$3E\% = \frac{\text{wt. of total drug} - \text{wt. of free drug}}{\text{wt. of total drug}} \times 100$$
 (1)

Zeta Potential (ζ)

The zeta potential of LGN-NLCs was measured using the Zetasizer NanoZS, which employs the Phase Analysis Light Scattering methodology, offering sensitivity up to 1000 times greater than conventional light scattering methods based on frequency spectrum shifts. The conductivity of the diluted samples was assessed to determine the detection model. The entire measurement was conducted at 25°C [17].

Optimized Formulation

The formula that showed the best result regrading to lower Particle Size and polydispersity

index and higher Entrapment Efficiency (EE%) was selected as optimized formula and furtherly optimized with different sonication times of 8, 10 and 15min. The formula with sonication time that showed the best results will be use as a selected formula.

Freeze-Drying of LGN-NLC

Lyophilization of LGN-NLCs selected formula was performed with mannitol as cryoprotectant at different ratios of 1.5, 3 and 5% w/v, using freeze dryer (Labconco, Canda), the obtained powder were stored in a tightly closed container for further investigations [14].

Microscopic Evaluation by Transmission Electron Microscopy (TEM)

The selected formula was examined for their morphology and size using TEM (model Zeiss Libra® 120 PLUS/ Carl Zeiss NTS GmbH/ Germany). The NLCs dispersion was applied on a carbon-coated copper grid, and the excess sample was drained off using filter paper. The sample allow for air dry and then the images of the sample were captured at an accelerating voltage of 21KV and the sample was viewed at suitable magnification power [18].

Evaluation of the Solid State Powder X-Ray Diffraction (PXRD) analysis

PXRD is used for the analysis of crystallinity of pharmaceuticals and excipients. The diffractograms can be used to determine whether the LGN present in the NLC samples is in crystalline or amorphous state. PXRD was applied using CuK α radiation with a wavelength of 1.5405 Å as the X-ray source. Samples were then placed in the glass holder and scanned from $2\theta = (5 \text{ to } 80)$, continuously. The operational voltage and current were maintained at 40 kV and 30 mA. Data were usually acquired every 0.05° using a detector with a resolution in the diffraction angle (2 θ) ranging from 10°C to 60°C at room temperature, including pure LGN samples, GMS, physical mixture, and LGN-NLCs [19].

Fourier Transform Infra-Red Spectroscopy (FTIR)

Fourier-transform infrared spectroscopy (FTIR) was utilized to identify potential interaction between LGN and other excipients, as well as to confirm drug identification. FTIR spectra were recorded for pure drug, Glyceryl monostearate,

J Nanostruct 16(1): 239-260, Winter 2026

(cc) BY

physical mixtures of drug and lipids and lyophilized LGN-NLCs, using FTIR Shimadzu (Model No. 8400S-Japan). The sample was weighed and formulated properly on KBr disk. The spectrum was recorded in the 4000–400 cm⁻¹ range with a spectral resolution of 4 cm⁻¹ [20].

Differential Scanning Colorimetry (DSC)

DSC allows anticipating the possible interactions between LGN and other excipients used in the research during the manufacture of LGN-NLCs by detecting the thermal characteristics of materials. Thermal analysis of pure LGN, GMS, and lyophilized LGN-NLCs. Samples of each were placed in standard aluminum pans and heated with a constant rate of 10°C/min in the temperature range of 30–300°C, using an empty aluminum pan as reference. The experiment was run under inert conditions with continuous nitrogen purging (30 ml/min) [21].

Evaluation of Powder Flowability Carr's Index (CI) and Hausner's Ratio (HR)

Five grams of lyophilized LGN-NLCs powder were placed in a 15 mL graduated cylinder, which was tapped 2-3 times to level the powder, and the initial untapped volume (V_o) was documented. Subsequently, the cylinder was manually tapped on a hard surface approximately 100 times, after which the final tapped volume (V_f) was recorded [22]. Carr's Index (Eqs. 2 and 3) and Hausner's ratio (Eqs. 2-4) were computed based on the values obtained from the tapping density tests (i.e., V_o and V_f).

Bulk density =
$$\frac{\text{Powder mass}}{\text{Bulk volume}}$$
 (2)

Tapped density =
$$\frac{\text{Powder mass}}{\text{Tapped volume}}$$
 (3)

(%) =
$$\frac{\text{Tapped density} - \text{Bulk density}}{\text{Tapped density}} \times 100$$
 (4)

$$HR = \frac{Tapped density}{Bulk density}$$
 (5)

Evaluation of Angle of Repose (එ)

The powder flow characteristics of the lyophilized LGN-NLCs were assessed by measuring the angle of repose (θ) via the fixed funnel and

free-standing cone technique. This method involves pouring powder through a funnel to create a cone, where the height of the cone (h) is divided by the radius (r) of its base and the inverse tangent of this ratio is designated as the angle of repose [23].

$$Tan(\theta) = \frac{h}{r} \tag{6}$$

Short term Stability Study of LGN-NLCs Optimized Formula

The short-term durability of the liquid LGN-NLCs examine under varying storage conditions, the optimized formula was distributed into two firmly sealed amber glass containers, with each container held at 25° C and 2-8° C for a duration of three months. The average P.S, PDI, and E.E% of the nanoparticles were assessed at 0, 45, and 90 days of storage, with results conducted in triplicate.

Ex-vivo Intestinal Permeation Study

Ex vivo permeation study of LGN-NLCs were conducted utilizing a modified non-everted rat gut sac method [24]. Two dispersed formulations containing an equivalent of 1mg for both optimized formula and 1mg LGN in 1mL normal saline were used as test and control, respectively. Male Sprague Dawley rats, weighing around 250-300 g, from the animal house in the College of Pharmacy/ University of Basrah were used in this study. The rats had an overnight fast with unrestricted access to water, followed by anesthesia with chloroform. Upon confirming the absence of pain reflex, a longitudinal abdominal incision was performed, and the small intestine was excised, with the mesentery manually peeled away [25]. The small intestine was cleaned out gently with cold normal saline solution using a syringe equipped with blunt end needle. The sanitized intestine was sectioned into sacs measuring 10 ± 0.2 cm in length and had a diameter of 0.25 cm. Upon securing one end with a silk suture, the intestinal sac was filled with 1 mL of the sample. Subsequently, the opposite end of the sac was tied, and the sac was immersed in a beaker containing 100mL of Kreb's-Ringer phosphate buffer saline at pH 7.4. The entire system was maintained at 37 \pm 1.0°C using a magnetic stirrer set to 100 rpm and constantly aerated with oxygen (60 bubbles/min). A 5 mL sample was extracted and substituted with Kreb's-Ringer solution at intervals of 30, 60, 90, 120, 150, 180, 210, and 240 minutes [26]. The released medication from one intestinal segment was quantified utilizing a UV spectrophotometer [27]. The apparent permeability coefficients were calculated utilizing Eq. 7 [28]:

$$Papp = \frac{F}{SA \times C^{\circ}}$$
 (7)

The (Papp, cm/min) is the apparent

permeability, (F, μ g/min) is the flux, (SA, cm2) is the area of the intestinal sac and (C°, μ g/ml) is the initial concentration of drug. The linear segment slope of the plot was considered as the permeation flux (F), (r) is the intestinal radius and (h) is the segment length.

RESULTS AND DISCUSSION

Determination of Solubility in Various Lipids
For a successful NLCs system formulation of

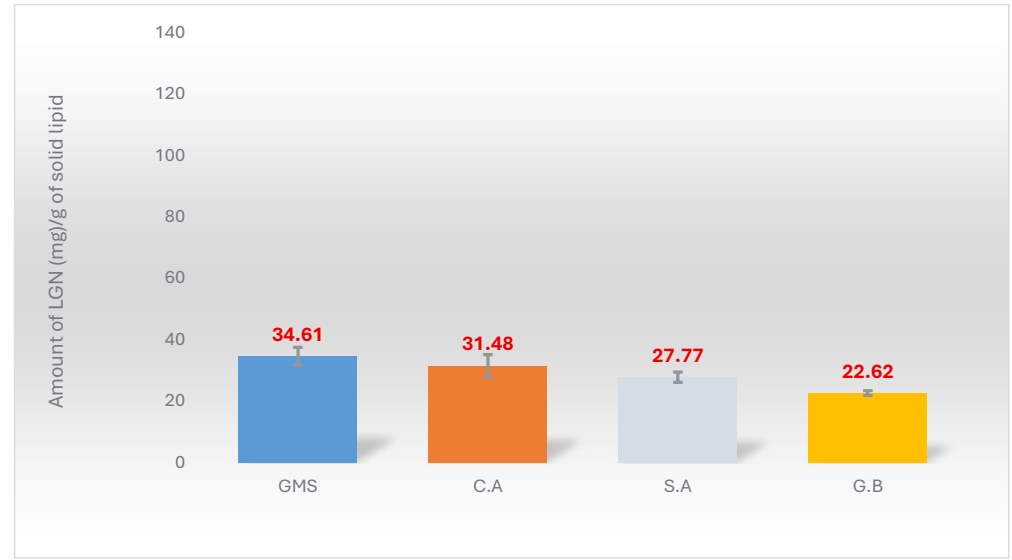


Fig. 1. Solubility of LGN in Solid Lipids.

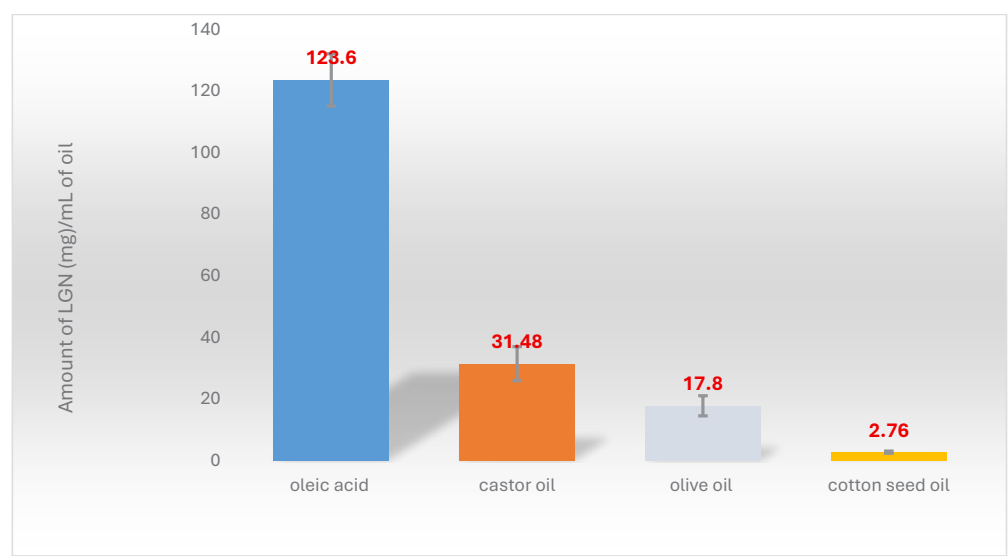


Fig. 2. Solubility of LGN in Liquid Lipids.

practically insoluble LGN, selection of suitable solid lipid and liquid lipid is essential to produce optimum drug loading. All excipients are of Generally Regarded as Safe (GRAS) grade were selected for NLCs fabrication [29].

Solubility in Solid Lipids

The solid lipids used to prepare the formulations should be considered to ensure high drug entrapment efficiency and loading capacity. This is because the appropriate lipid matrix selection enhances the physical and chemical stability of

the entrapped drug [30]. As shown in Fig. 1, the solubility of LGN in GMS, cetyl alcohol, stearic acid and glyceryl behenate were found to be 34.61 \pm 0.076 mg/g, 31.48 \pm 0.061 mg/g, 27.77 \pm 0.094 mg/g, and 22.62 \pm 0.057 mg/g respectively. Thus, GMS was chosen as the lipid phase for LGN - NLCs formulation [31].

Solubility in Liquid Lipids

As shown in Fig. 2, the oil solubility study of LGN shows that oleic acid has a better solubility for LGN compared to other oils explored in this

 $\underline{ \text{Table 2. Particle size. Polydispersity Index and Entrapment Efficiency \% of LGN-NLCs (Mean <math>\pm$ SD (n=3).}

F	Average particle size(nm)	Polydispersity Index	Entrapment Efficiency %
1	175.4 ± 3.16	0.382 ± 0.012	66.8± 2.74
2	119.9 ± 7.12	0.324 ± 0.009	70.2 ± 2.6
3	119 ± 6.79	0.314 ± 0.008	72.4 ± 3.96
4	112.5 ± 2.14	0.301 ± 0.036	84.5 ± 3.65
5	127.1 ± 9.3	0.382 ± 0.043	67.81 ± 0.54
6	122.4 ± 3.65	0.357 ± 0.019	69.2 ± 2.21
7	62.86 ± 4.41	0.314 ± 0.011	72.24 ± 4.23
8	46.13 ± 2.19	0.279 ± 0.026	79.75 ± 0.87
9	117.8 ± 1.86	0.338 ± 0.038	69.57 ± 3.76
10	115.1 ± 9.54	0.247 ± 0.002	68.8 ± 2.43
11	112.8 ± 1.56	0.281 ± 0.008	71.1.4 ± 2.54
12	71.56 ± 6.79	0.216 ± 0.003	73.78 ± 2.73
13	113.6 ± 7.56	0.441 ± 0.038	76.55 ± 1.76
14	85.29 ± 5.18	0.384 ± 0.017	72.35 ± 2.1
15	71.5 ± 3.9	0.298 ± 0.033	74.08 ± 4.1
16	71.39 ± 4.52	0.274 ± 0.005	81.7 ± 0.86
17	407.34 ± 19.21	0.422 ± 0.037	64.91 ± 3.9
18	357.12 ± 12.5	0.373 ± 0.033	67.44 ± 5.3
19	316.81 ± 17.52	0.336 ± 0.005	65.14 ± 3.48
20	247.77 ± 14.07	0.352 ± 0.026	72.68 ± 2.98
21	362.51 ± 29.89	0.294 ± 0.006	70.74 ± 1.9
22	273.17 ± 15.86	0.413 ± 0.041	66.19 ± 1.32
23	216.6 ± 12.43	0.469 ± 0.039	76.83 ± 3.1
24	167.19 ± 6.75	0.37 ± 0.027	80.34 ± 6.25
25	223.24 ± 11.3	0.437 ±0.053	82.8 ± 3.81
26	207.87 ± 9.87	0.343 ± 0.002	84.91 ± 2.23
27	289.67 ± 21.42	0.384 ± 0.009	85.07 ± 1.13

research like castor oil, olive oil and cottonseed oil. Oleic acid shows significantly better solubility for LGN than other oils resulting from optimal solubilization ability likely due to the hydrogen bonds formed by the carboxylic group of fatty acids with drug molecules. Therefore, it was chosen to be the liquid lipid for the LGN-NLCs formulation [32].

Preparation

LGN-NLCs were effectively prepared using melt emulsification and ultrasonication. Optimization was done on several formulation parameters, such as adding melted lipid phase to the aqueous phase at ~1 mL/min dropwise. After dispersing each drop in the aqueous surfactant solution, add the next and stir thoroughly. During LGN-NLCs preparation, all lipids produced a transparent microemulsion at 70°C. However, upon chilling, lower temperatures caused turbidity and solidification, resulting in a translucent dispersion upon warming. Table 2, shows the mean particle size distribution, polydispersity index, and entrapment efficiency of the LGN-NLCs.

Characterization of prepared LGN-NLCs Particle Size Distribution and Polydispersity Index

Most of the prepared LGN-NLCs had particle sizes in the sub-micrometer region (Table 2). Particle size analysis is crucial for the characterization of lipid nanoparticles as the drug pharmacokinetics, the tissue-distribution, elimination, and clearance

of the drug all are influenced. A particle size of ≤100 nm seems to be the most effective for intestinal uptake of nano-structured lipid carriers (NLCs) [33].

In lipid-based drug delivery systems, a PDI of 0.3 or less is considered ideal as a system is homogeneously dispersed [34]. The PDI of most of the developed LGN- NLCs was less than 0.4 denoting a narrow size distribution.

Effect of Surfactant Type and Concentration

Our study demonstrated that, as the surfactant content increased, the particle size of the formed LGN-NLCs was decreased. The reduction in the particle size was seen on increasing the concentration of tween 80, where the size of F1 that have 1% w/v tween80 was 127±6.79 nm reduced to 112.5±7.13 nm when concentration of tween 80 rise to 2.5% w/v in F4. The Tween 80 amount has significant (p<0.05) effect on particle size and polydispersity index of the formulated NLCs. This may be due to the lack of surfactant molecules at low concentrations of surfactant to fully coat the new hydrophobic surfaces created during the solidification of the lipid matrix [35].

The results are shown in Fig. 3A. When the concentration of the lipophilic surfactant span80 was increased from 1% in formula F17 up to 2.5% in formula F20 a significant decrease in the particle size (p<0.05) from 407.34 ± 19.21 nm (F11) to reach 247.77 ± 14.07 nm and PDI was approximately \leq 0.4 in all the concentrations of



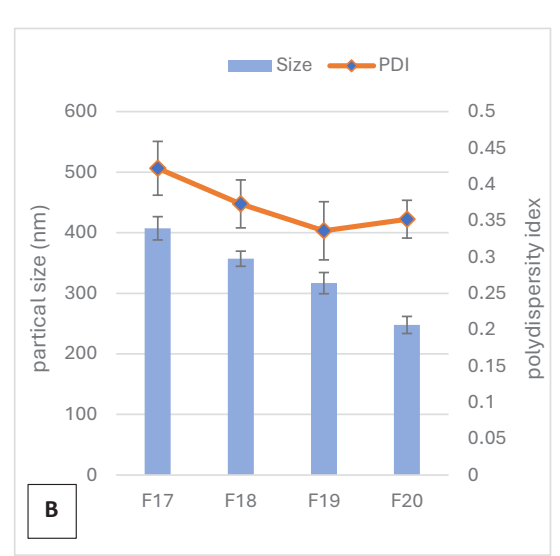


Fig. 3. The effect of (A)- Tween 80 concentration, (B)- Span 80 concentration on the particle size distribution and PDI of LGN-NLCs.

span80 as shown below in Fig. 3B.

Effect of Co-surfactant Type and Concentration

A co-surfactant is required for the preparation of a homogeneous dispersion of NLCs as the use of surfactants only suppress the interfacial tension between melted lipid droplets and the aqueous phase to a limited extent [36]. As such, the role of a co-surfactant is important for enabling the facile preparation of stable LGN-NLCs. PEG400 was a co-surfactant in the present study. It can be observed from the results in Fig. 4, that when the PEG 400 concentration is increased from 1% to 2.5%, there are significant decreases in particle size and PDI

of the LGN-NLCs (p<0.05). It is suggested that the particle size decrease may be due to the interaction of PEG400 with the surfactant molecules at the interface of the lipid nanodroplets decreasing interfacial tension and consequently lowering the possibility of nanoparticle coalescence and increasing the overall system stability. Similar results were also found by Liu et al. and his coworkers [37].

The influence of different co-surfactants (PEG400, PEG600, PEG200, and Propylene glycol) was tested on the particle size of LGN-NLCs in formulas F8, F21, F22 and F23 respectively. As revealed from the data in Table 2, the type of co-

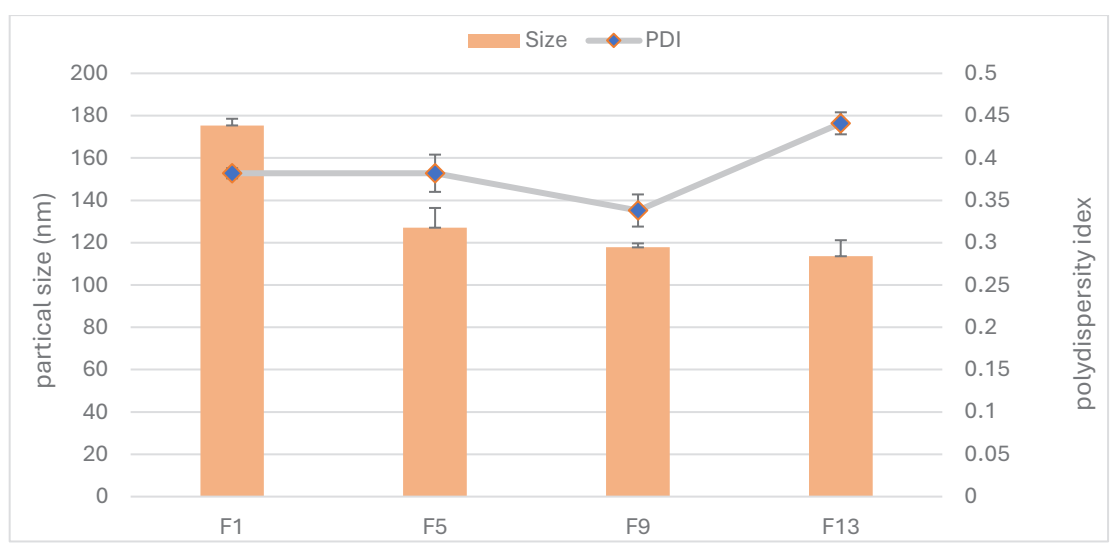


Fig. 4. The effect of PEG-400 concentration on the particle size distribution and PDI of LGN-NLCs.

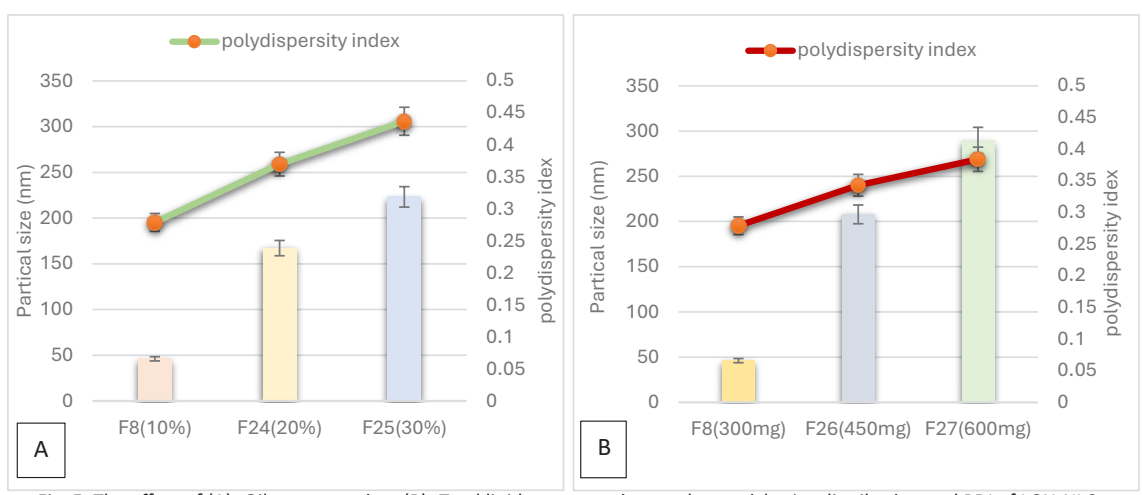


Fig. 5. The effect of (A)- Oil concentration, (B)- Total lipid concentration on the particle size distribution and PDI of LGN-NLCs.

surfactant had a significant effect on the particle size distribution (p<0.05). PEG-400 offers the smallest particle size (46.13 \pm 2.19 nm) among the employed co-surfactants, thus proving effective co-surfactant to produce relatively uniform dispersion of LGN-NLCs.

Effect of Liquid Lipid Type and Ratio

When the ratio of oleic acid to GMS was increased from 10% in the formula F8 to 20% and 30% in the formula F24 and 25 we found an increase in the particle size from (46.13 \pm 2.19 nm) of F8 to (223.24 \pm 11.3 nm) of F25. This agrees with the claim that at higher than 10% concentration of oleic acid, the particle size will be increased with more oleic acid adding into the core of the oleic acid loading nanoparticles. This same observation

was reported by Dai et al. and his co-workers [38]. Therefore, increasing the ratio of liquid lipid beyond 10% has a significant effect (p<0.05) on the particle size of the PGN-NLCs, and the effect on the particle size distribution can be observed from Fig. 5A by increasing oleic acid ratio.

Effect of Drug to Lipid Ratio

Increasing the lipid to drug ratio from 300mg of total lipid in formula F20 up to 450mg and 600mg in formulas F26 and F27 respectively shows a significant increase in the particle size and the polydispersity index (P<0.05), When the amount of solid lipid increases at a fixed concentration of surfactant, it is difficult for surfactant molecules to cover the entire surfaces of the lipid droplets, resulting in aggregation of the particles and an

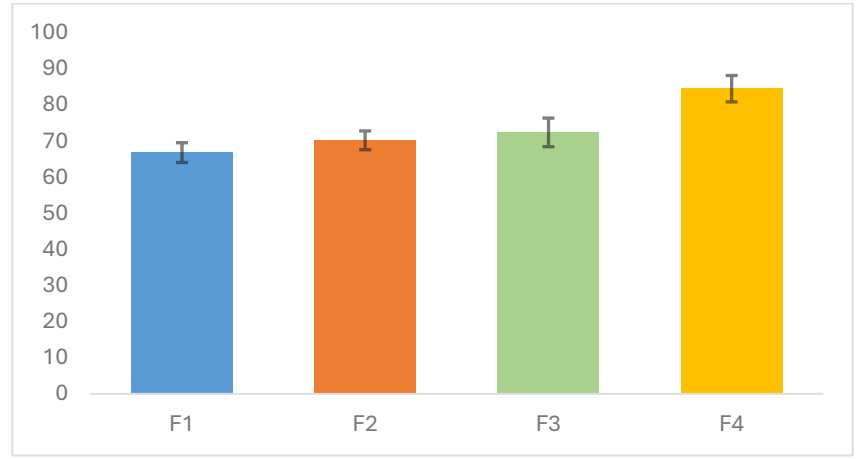


Fig. 6. Effect of Tween 80 concentration on %EE of LGN-NLCs.

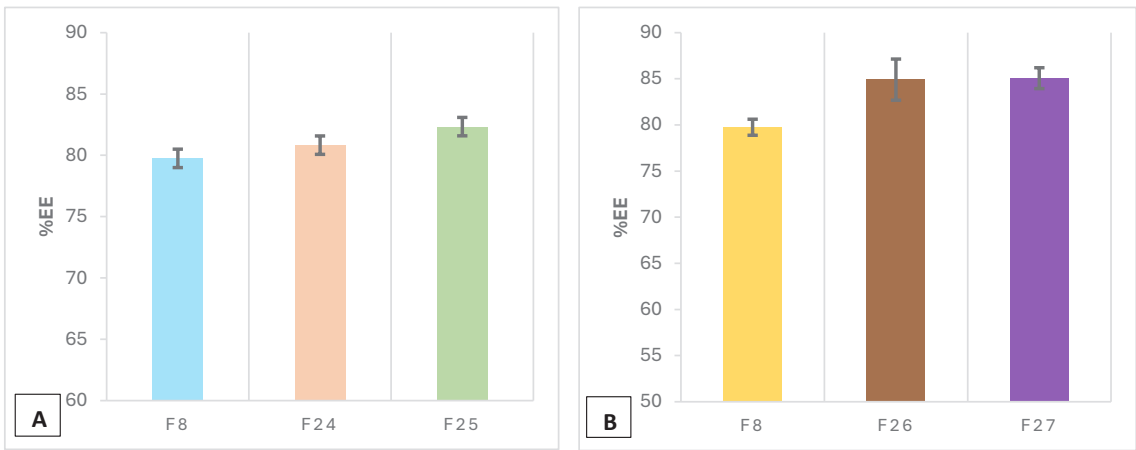


Fig. 7. The effect of (A)- Liquid lipid ratio, (B)- Solid lipid ratio on %EE of LGN-NLCs.

increase in both particle size and dispersity. A similar observation was described by Dandagi et al. [39], the effect of lipid ratio on particle size distribution was shown in Fig. 5B.

Entrapment Efficiency

Entrapment efficiency (%EE) refers to the proportion of the drug effectively integrated into the lipid matrix of the nanoparticles relative to the total drug quantity introduced during the lipid nanoparticle manufacturing process [40]. They constitute essential parameters in the formulation owing to their impact on drug release characteristics and, therefore, its bioavailability to the biological system. Hydrophobic drug molecules are incorporated into NLCs with more efficiency than hydrophilic pharmaceuticals, since

the latter tend to partition into the aqueous phase during homogenization, leaving the lipid phase [41]. The current study achieved a satisfactory encapsulation efficiency (%EE) for the majority of the formulated LGN-NLCs, likely owing to LGN's good affinity for the lipid matrix, as shown by its lipophilic partition coefficient (logP: 1.9) [42].

An apparent increase of entrapment efficiency was found when the concentration of the various surfactants was increased from 1% to 2.5%, with a 2.5% concentration of surfactant revealing the highest %EE for all formulations. The %EE of most of the prepared LGN-NLCs are acceptable, which may be due to a good solubility of the drug in solid and liquid lipids (used in the production method) and its low aqueous solubility. As a consequence of this, the %EE depends mainly on the

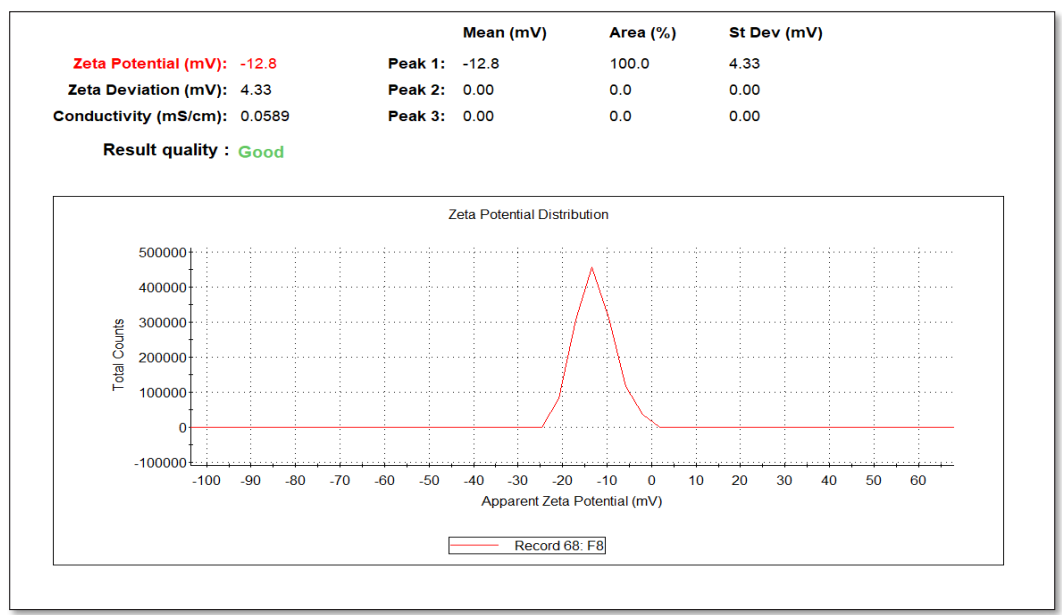


Fig. 8. Zeta potential of LGN-NLCs of optimized formula (F8).

Table 3. The Effect of Sonication Time on the Particle Size Distribution of LGN-NLCs F8, Mean values ±SD (n=3).

	Sonication time			
Time (min)	8	10	15	
P. S	62.86 ± 4.41	46.13 ± 2.19	44.73 ± 2.72	
PDI	0.314 ± 0.011	0.279 ± 0.026	0.259 ± 0.0079	

physicochemical properties of the encapsulated drug and the lipid phase applied [43].

Increase in the oleic acid content (at 10% and then 20% and 30% of the total lipid) for F20, F24, F25, respectively in Fig. 7A led in modest increase in %EE. This result can be explained by the presence of more imperfections on the lipid structure, which enables the entry of a higher

amount of drug molecules in the nanoparticle and because the solubility of the drug in oil is greater than in solid lipid, as observed by Le-Jiao Jia et al.

The higher percentage of entrapped drug was obtained by increasing the ratio of GMS because of its high level of mono-, di-, and triglycerides which also improve the solubility of the lipophilic drug

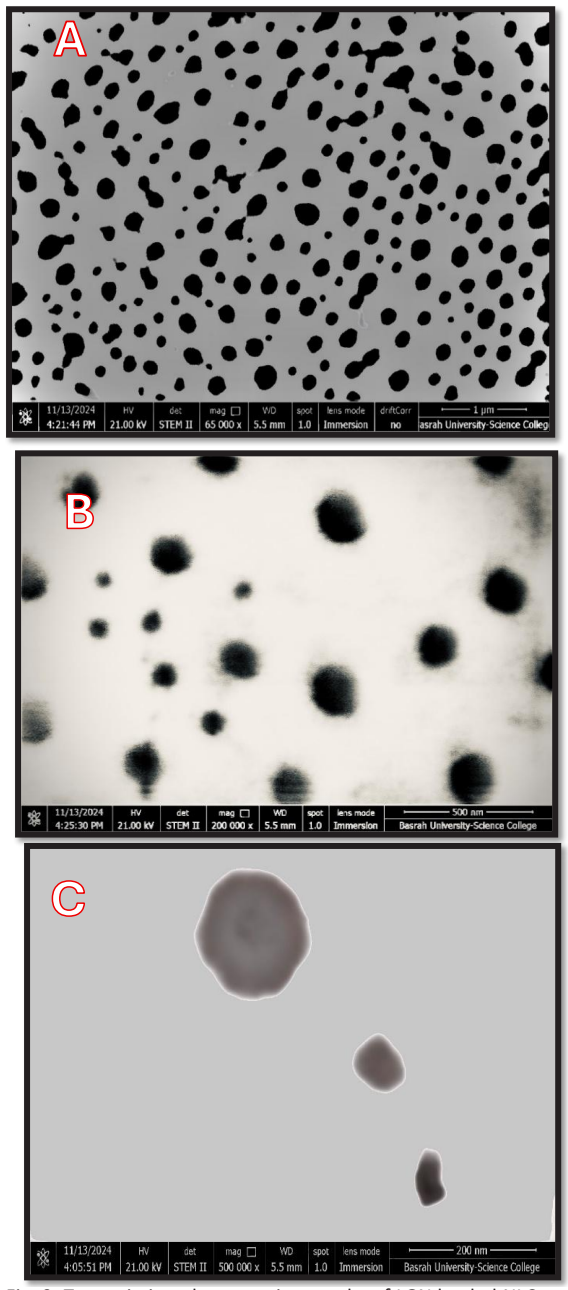


Fig. 9. Transmission electron micrographs of LGN loaded NLCs at magnification powers (A-65,000, B-200,000 and C-500,000.

[45]. statistically significant difference (p<0.05) in EE% was observed between F8 and both F26 and F27 while the increase in the EE% between F31 and F32 was non-significant (P>0.05) indicated that there was no extra benefit from further increase in lipid ratio. Similar results were presented by Sangsen et al. [46], results were shown in Fig. 7B.

Zeta Potential (ζ)

The assessment of zeta potential (ZP) values of the formulated LGN-NLCs is a critical factor in evaluating the long-term stability of the system during storage. The measurement of electrical potential at the particle shear plane indicates that a larger ZP value correlates with increased stability of the colloidal system, as it enhances repulsion between proximate, similarly charged particles, hence preventing particle aggregation [47]. In Fig. 8 showing formula F8 utilizing 2.5% Tween 80 as a surfactant, Zeta Potential peaking at -12.8 mV. This negative charge on the particles provides stability preventing and their aggregation due to electrostatic repulsion. On the other hand, Tween 80 being a non-ionic surfactant, provides stabilization by steric repulsion [48].

Selection of Optimized Formula

Regarding to the data resulted from

determination of particle size, polydispersity index, zeta potential, drug entrapment efficiency the formula F8 was selected as the best formula. It shows particle size of (46.13 nm) and PDI of (0.279) and a zeta potential of (-12.8 mV), with drug entrapment of (79.75 %).

Effect of Sonication Time

Formula F8 was employed to investigate the impact of sonication duration on particle size distribution, revealing a significant reduction (p <0.05) in mean particle size and polydispersity index after extending the sonication time to 10 min. Conversely, at a 12min sonication duration, a slight increase in particle size was noted (p > 0.05), as illustrated in Table 3. Prolonged sonication duration delivers more energy to disintegrate the particles. Consequently, smaller particles were produced as the duration of sonication increased which directly influences the final dispersion particle size. Nevertheless, the decrease in size was minimal after 10 minutes of sonication duration [49].

Microscopic Evaluation by Transmission Electron Microscopy (TEM)

Imaging Transmission electron microscopy (TEM) is commonly used method for the analysis

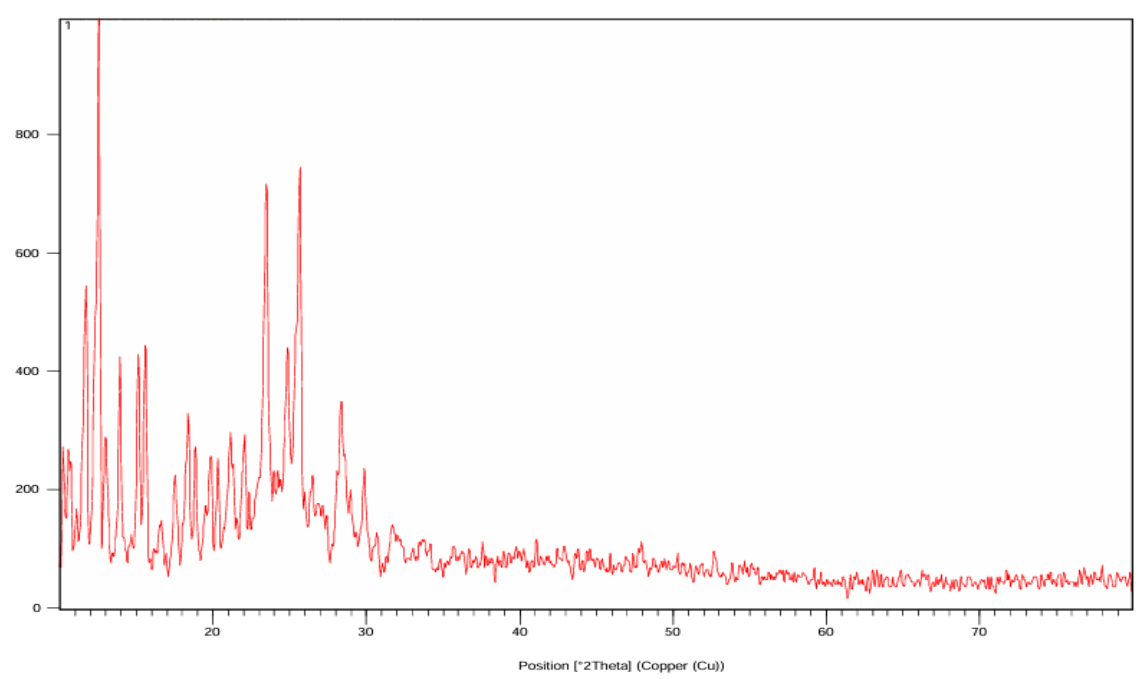


Figure 10: PXRD pattern of pure linagliptin.

and visualization of subjects in the nanoscale size range in a higher resolution compared to other techniques because it utilizes a high energy electron beam with a shorter wavelength than light [50]. A TEM study of the selected formula F8 reveals that LGN-NLCs particles were almost spherical in shape with smooth surfaces and their particle sizes are within the nanoscale range and no particle aggregation was observed as seen in Fig. 9 A, B and C.

Evaluation of the Solid State

Powder X-ray Diffraction Analysis (PXRD)

We now compared the XRD patterns from pure

LGN, GMS, a physical mixture of LGN and GMS and LGN-NLCs. It was demonstrated that the XRD pattern of pure LGN in Fig. 10 contained sharply crystalline structures characterized by several sharp peaks with strong diffraction intensities which appeared at the angles 20– 4.4710°, 23.5469° and 25.6282°. The diffraction pattern produced by the physical mixture was strikingly different from that for LGN-NLCs. The diffraction peaks were obtained at 20 values of 18.5057°, 23.8859°, and 38.7918° as depicted in Fig. 11 together with the diffractogram of GMS in Fig. 12. But these signature peaks disappeared, and their intensity reduced dramatically relative to

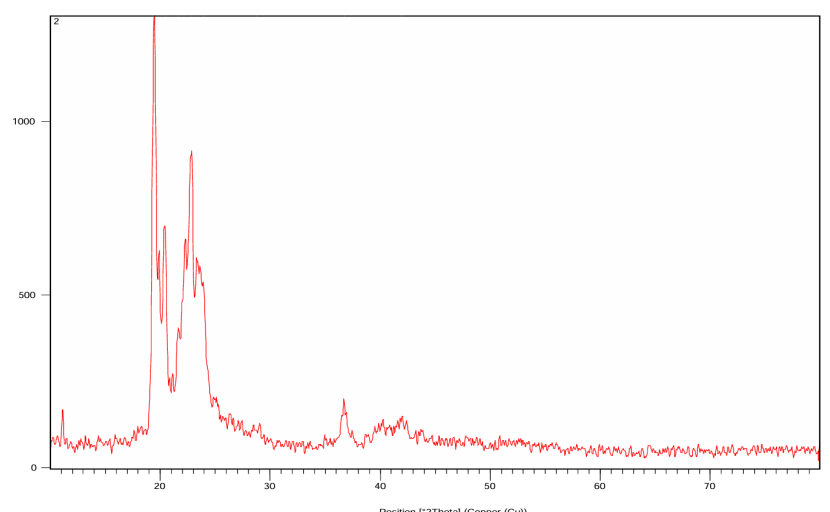


Fig. 11. PXRD pattern of Glyceryl monostearate.

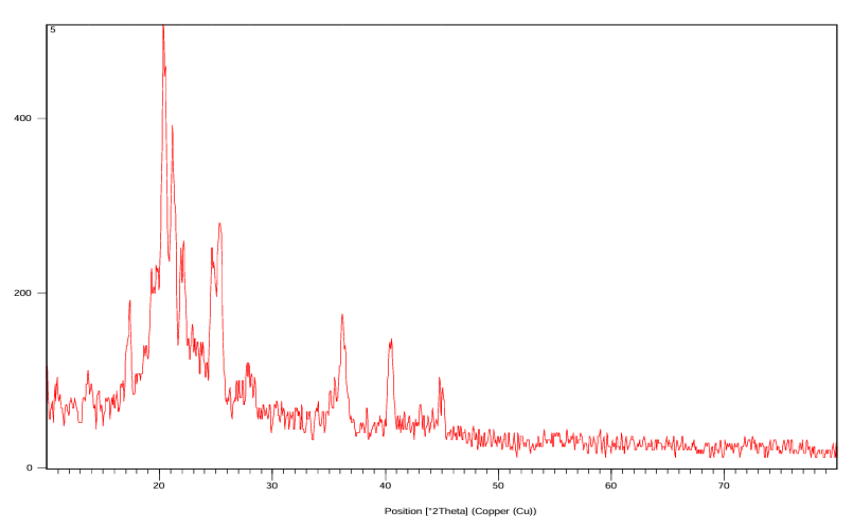


Fig. 12. PXRD diffractogram of physical mixture (LGN + GMS).

LGN-NLCs, as illustrated in Fig. 13. Furthermore, the PXRD results showed the GMS reveals a random crystallin in the NLCs. There is absence of characteristic peaks for LGN in the diffractogram of the optimized NLCs, indicating that LGN is either amorphous or molecularly dispersed (probably because it is entrapped in the lipid matrix of the nanoparticle dispersion formed).

Fourier Transform Infra-Red Spectroscopy (FTIR)

FTIR spectroscopic study is important to check the compatibility of the drug with other excipients and is one of the basic criteria in selection of better excipients. FTIR is a powerful technique for evaluating possible structural alterations of the drug due to harsh and stressful situations faced during the formulation process. Figs. 14-16 display FTIR spectra of pure LGN, GMS, the physical mixture, and drug-loaded NLCs, respectively.

The spectrum of LGN (Fig. 14) presented typical peaks due to the carbonyl group (C=O stretching) in purine ring at 1695.14 cm⁻¹ and 1652.02. Also, A peak at 3356.41 cm⁻¹ (N-H stretching) overlaps with (N-H) stretching of the piperidine group, Peak at 1566 cm⁻¹ constitutes (N-H bending of amide), peak at 1502 cm⁻¹ signifies (C=C aromatic). In

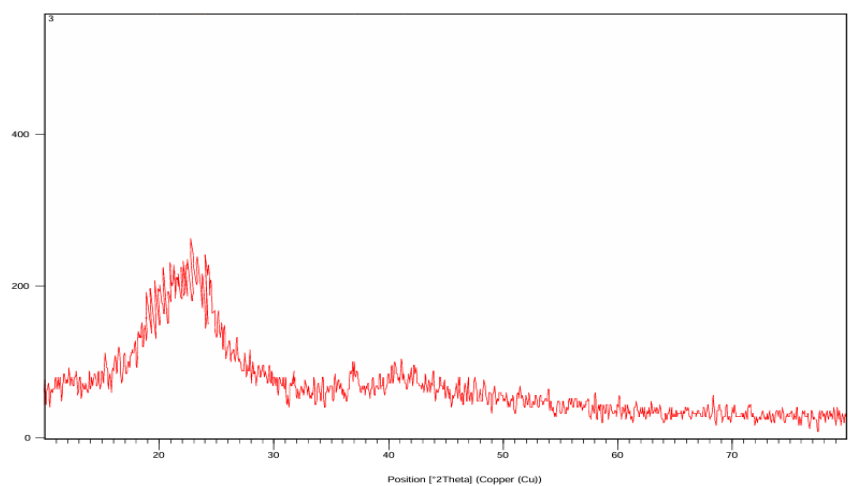


Fig. 13. PXRD diffractogram of lyophilized LGN-NLCs of optimized formula (F8).

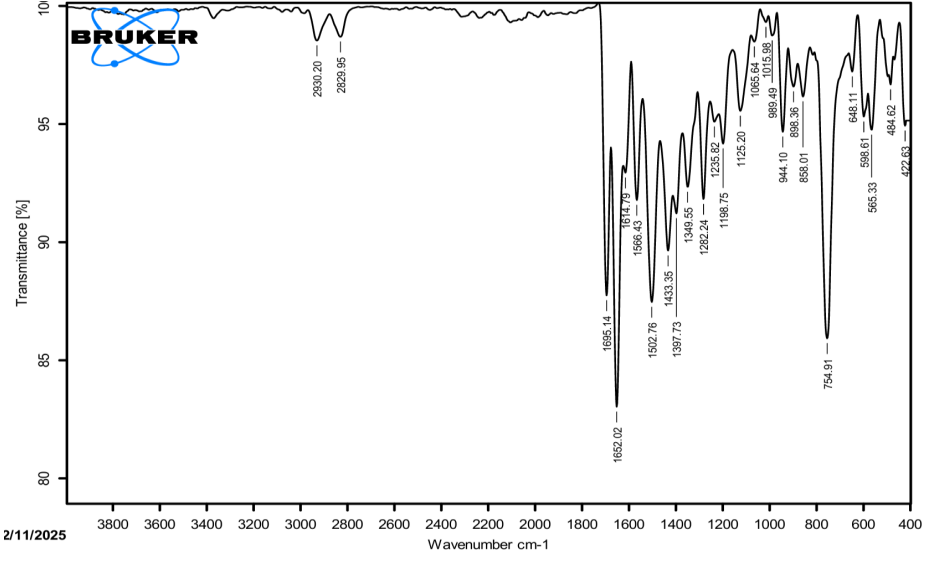
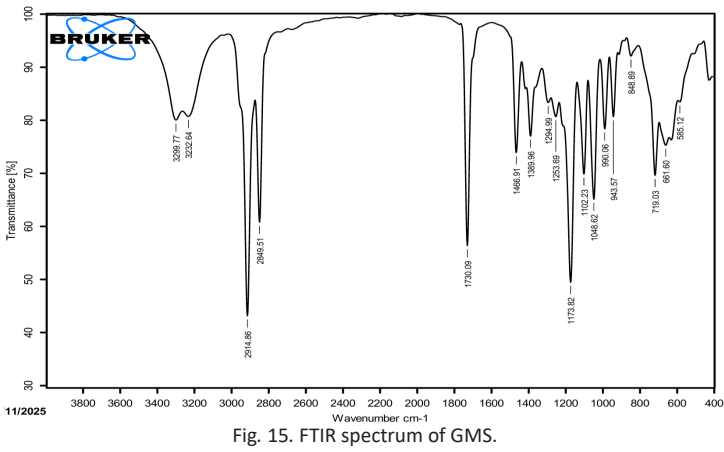
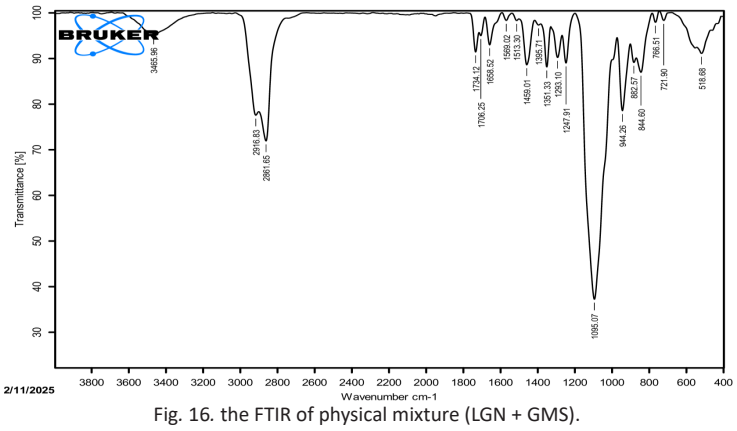


Fig. 14. FTIR spectrum of pure linagliptin.

addition, the two peaks were detected at 2829.95 cm⁻¹ and 2930.2 cm-1 which indicated the (C-H stretch) of alkane groups. The peaks observed IR spectra confirm the purity of the drug [51].

The IR spectrum of GMS was shown in Fig. 15 exhibited broad two peaks at 3299.77 cm⁻¹ and





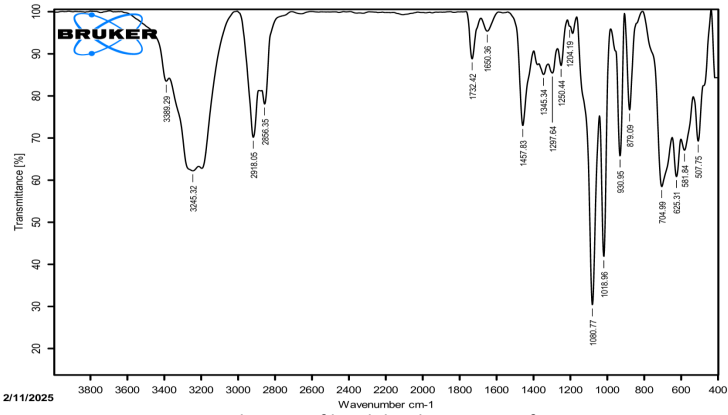


Fig. 17. The FTIR of lyophilized LGN-NLCs of F8.

3232.64 cm⁻¹ indicating (O-H) stretching of glycerol moiety, two peaks that are at 2914.86 and 2849.51 cm⁻¹. These peaks are due to (C-H) stretching of alkane, the carboxyl group (C=O) stretching peak is observed at 1730.09 cm⁻¹ and strong peak at 1173.82 cm⁻¹ for (C-O) stretching of ester [52].

FT-IR spectrum of F8 showed fewer LGN peaks

(Fig. 17), signifying a higher entrapment of LGN in the lipid matrix. However, no shifting of specific peaks was observed, and these peaks were present in their respective positions in the individual spectra, suggesting no interaction of the drug and the excipient. The preparation process was not affecting the molecular structure and the chemical

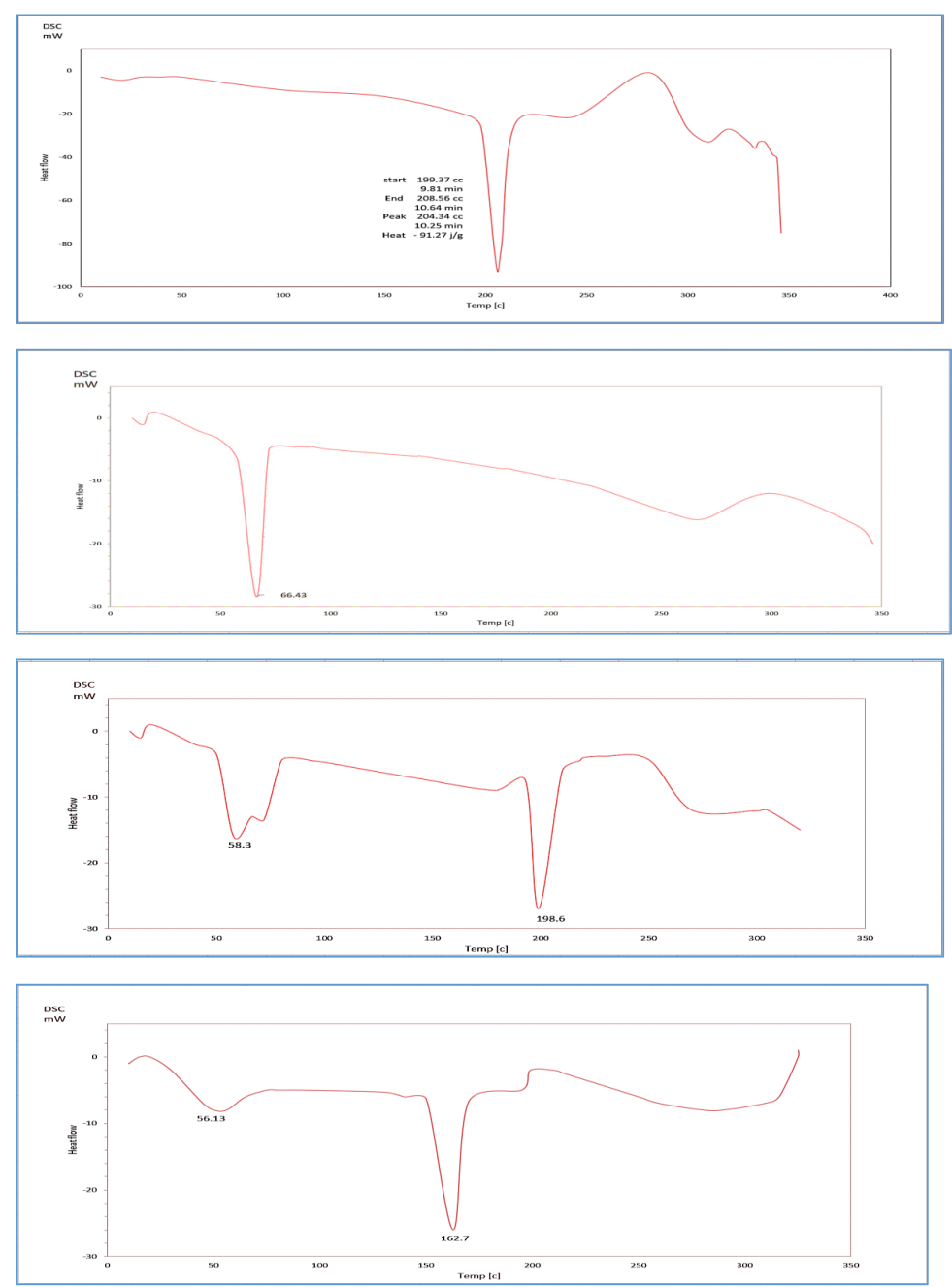


Fig. 18. DCS thermogram (A) linagliptin, (B) GMS, (C) physical mixture (LGN + GMS) and (D) lyophilized LGN-NLCs of optimized formula (F8).

integrity of LGN. Thus, FTIR spectroscopy serves as additional evidence of interactions between LGN and various excipients (lipids, stabilizers, etc.) prior to and post formulation.

Differential Scanning Calorimetry Study (DSC)

The thermal properties of the LGN, GMS, their physical mixture, and lyophilized optimized formula (F8) were evaluated by DSC, which was shown in Figs. 18, A-D.

The DSC thermograms of pure drug (Fig. 18A) shows a sharp endothermic peak at 204.45°C, attributed to its melting point; so it expresses that LGN is pure and in crystalline anhydrous form [51]. Fig. 18B shows the thermogram of GMS where endothermic peak with at 66.43°C was observed, indicating a very high ordered molecular structure.

The thermogram of physical mixture (Fig 18C) also shows the endothermic peaks of GMS and LGN indicating their compatibility and crystalline nature. The fact that no endothermic peak of the drug was detected from the LGN-loaded NLCs (F8) thermogram (Fig. 18D) proved that the drugs were entrapped in the matrix and are present in the amorphous phase. This can be due to the fast cooling of a hot nanoemulsion to form the NLC whereby the drug does not crystallize at this drug level in this case. Moreover, the surfactant will also inhibit the medicament to crystallize [53].

Furthermore, it was observed that the melting endotherm of bulk GMS decreased to 56.13°C during LGN-NLC, and this reduction in melting endotherm has been attributed to heterogeneity in content of NLCs such as solid lipid, oil and drug which are encapsulated into the particle. These

defects in solid lipid structure with molecular distribution of the added oil throughout the lipid blend led to decreased crystallinity of the solid lipid and drug molecules and distortion of the solid lipid matrix [54].

New endothermic peak at 162.7°C representing the melting endotherm of mannitol that used as lyoprotectants in freeze drying process [55].

Short Term Stability Study

A stability investigation was performed at two distinct storage temperatures: 2-8°C (refrigerator) and 25°C during a duration of ninety days. Samples were collected at the initiation of the study (day zero), the midpoint (day 45), and the conclusion (day 90). The measurements of particle size, polydispersity index (PDI), and percent entrapment efficiency (%EE) were documented. The results collected are presented in Table 4 below:

The particle size distribution results indicate a substantial increase in particle size and polydispersity index (PDI) at a storage temperature of 25°C (p<0.05) by the conclusion of the study, in comparison to measurements taken on day zero. The rate of particle growth was more pronounced at 25°C than at 2-8°C, which exhibited minimal alterations in particle size and PDI. Notably, flocculation was observed on the 30th day of storage at 25°C, corroborating the findings of Hu et al. [56]. This can be elucidated by the fact that elevated temperatures result in increased energy, which in turn raises the rate of collisions between particles and therefore enhances the likelihood of particle aggregation [57].

Table 4. Physical Characterization of LGN-NLCs after Short-Term Stability Study, Results Mean ±SD (n=3).

Time	Day zero		Day 45 th		Day 90 th	
Temp.	0-8 C°	25 C°	0-8 C°	25 C°	0-8 C°	25 C°
P. S	46.13 ± 2.19	46.13 ± 2.19	47.09 ± 1.8	73.55 ± 1.19	51.62 ± 2.51	110.81 ± 2.87
PDI	0.279 ± 0.03	0.279 ± 0.03	0.297 ± 0.01	0.318 ± 0.04	0.321 ± 0.026	0.345 ± 0.037
E.E%	79.75 ± 0.87	79.75 ± 0.87	77.14 ± 0.63	75.54 ± 1.3	76.39 ± 0.97	71.92 ± 2.23

Ex-vivo Study Using the Non-Everted Intestinal Sac Model

The non-everted intestinal sac technique was employed in this study owing to its numerous advantages over alternative technique, such as reduced structural damage to intestinal tissue compared to the everted sac model, an easier and more accessible procedure, reduced test

sample requirements, and facilitated collection of consecutive serosal test samples. Fig. 19 illustrates the quantity of LGN permeate from the optimized formula F8 and the control in the jejunum segments utilized in the investigation.

By assuming the intestinal segments as a cylinder with a mean diameter of 0.25 cm and a length of 10 cm, the surface area of the gut sac may

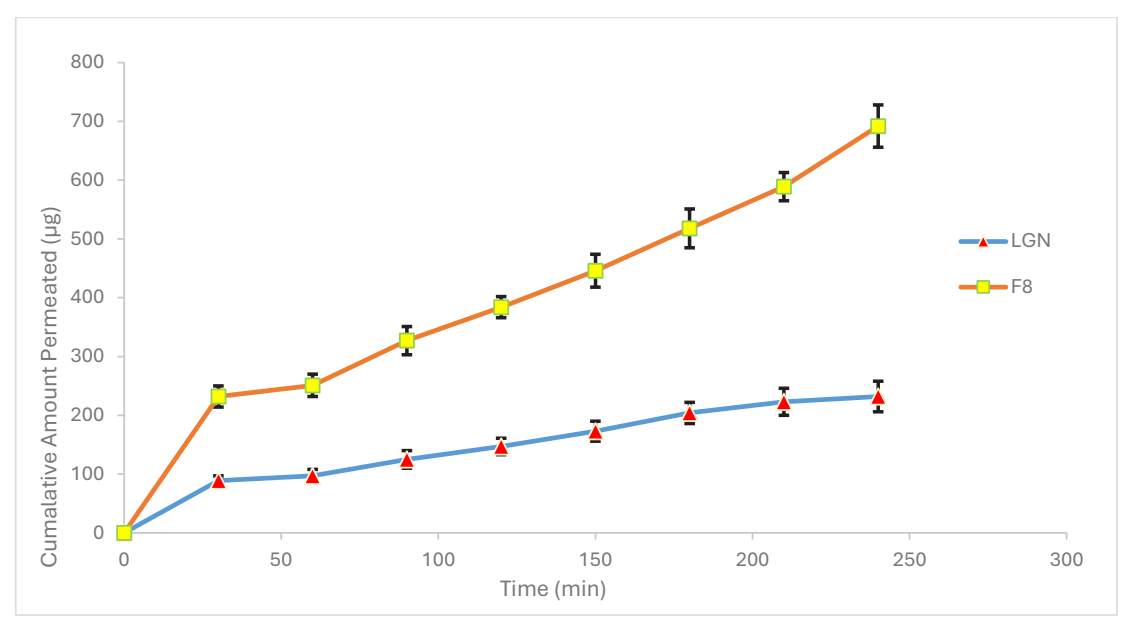
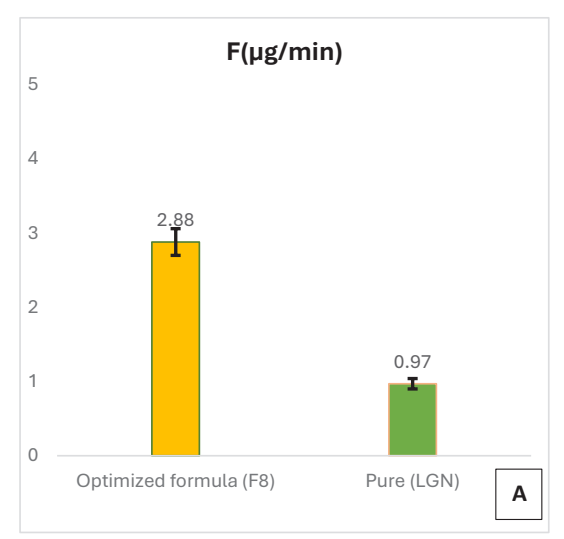


Fig. 19. Permeation of linagliptin from optimized formula F8 and control through non-everted rat duodenum, values of mean ±SD (n=3).



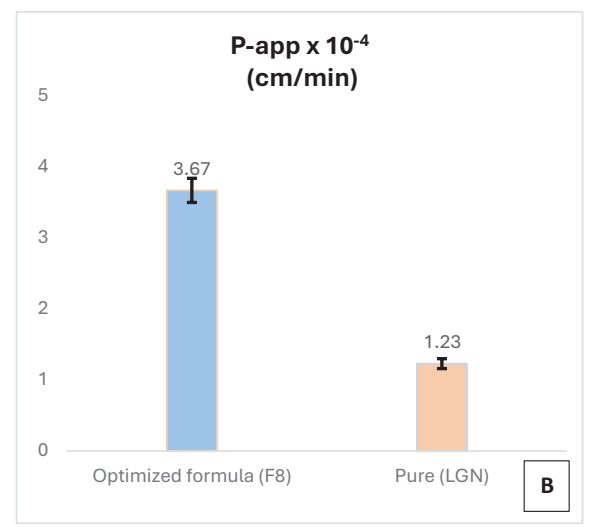


Fig. 20. A)-The permeation rate (flux) and (B)-The permeability coefficient(cm/min) of LGN and LGN-NLCs.

be readily calculated. The intestinal permeability results indicated that the tested LGN-NLCs formula F8 demonstrated significantly greater intestinal permeability than the control (p <0.05). The flux (µg/min) of LGN derived from formula F8 in Fig. 20A was determined to be 2.88 ± 0.18 from jejunal segments, while the flux for pure drug suspension was 0.97 ± 0.074 from the jejunum. The apparent permeability coefficient (cm/min) for the optimal formula F8 Fig. 20B was determined to be 3.67 ± 0.26 , while the value for the pure drug suspension was 1.23 ± 0.069 for the jejunum, indicating a threefold enhancement in drug permeability from LGN-NLC relative to pure LGN suspension.

The observed results may be attributed to several factors: the diminutive particle size and significant adhesion resulting from the large surface area, which facilitate increased drug diffusion and dissolution, potentially explaining the augmented drug penetration [58, 59]. The application of permeability-enhancing excipients, such as Tween 80 and oleic acid, which reduce intestinal P-glycoprotein efflux pump activity, likely enhances drug permeability [60, 61]. The LGN-loaded NLCs significantly contribute to drug protection and the regulation of drug release, leading to enhanced penetration across the intestinal barrier [62].

CONCLUSION

LGP-NLCs were effectively synthesized by the modified hot emulsification-ultrasonication technique and optimized via a 27 formulation. LGP-NLCs were characterized using DLS, XRD, FTIR spectroscopy, DSC, and TEM techniques. The nanometric range of size indicated targeting of intestinal lymphatics. Rat noneverted sac permeability tests demonstrated that the incorporation of P-glycoprotein inhibitors such as oleic acid and Tween 80 in lipid-core nanostructured lipid carriers enhanced the absorptive transport of LGP NLCs compared to LGP-SOL. The enhanced bio-absorption would result in a decrease in dosage, NLCs represent promising vehicles for the oral delivery of the novel anti-diabetic agent LGP; however, clinical trials are necessary to validate the proof of concept.

CONFLICT OF INTEREST

The authors declare that there is no conflict of interests regarding the publication of this manuscript.

REFERENCES

- Barati S, Yadegari A, Shahmohammadi M, Azami F, Tahmasebi F, Rouhani MR, et al. Curcumin as a promising therapeutic agent for diabetic neuropathy: from molecular mechanisms to functional recovery. Diabetology and Metabolic Syndrome. 2025;17(1).
- Hay-Bradford EJ. Pharmacological Interventions for Diabetes Management. The Pharmacist's Pocket Guide for Diabetes and Obesity: Springer Nature Switzerland; 2025. p. 69-108.
- 3. Parthasarathi V, K H. Dipeptidyl Peptidase-4 A Comprehensive Review. Current Enzyme Inhibition. 2025;21.
- 4. Jain A, Vispute A, Dange A, Naskar A, Mondal A, Vivekanand B, et al. A Randomized, Double-Blind, Parallel-Group Phase III Trial Investigating the Glycemic Efficacy and Safety Profile of Fixed-Dose Combination Dapagliflozin and Linagliptin Over Linagliptin Monotherapy in Patients with Inadequately Controlled Type 2 Diabetes with Metformin. Diabetes Ther. 2023;15(1):215-227.
- Aljohani H, Alrubaish FS, Alghamdi WM, Al-Harbi F. Safety of Linagliptin in Patients with Type 2 Diabetes Mellitus: A Systematic Review and Meta-analysis of Randomized Clinical Trials. Therapeutic Innovation and Regulatory Science. 2024;58(4):622-633.
- Shaik M, Vanapatla SR. Enhanced oral bioavailability of linagliptin by the influence of gallic acid and ellagic acid in male Wistar albino rats: involvement of p-glycoprotein inhibition. Drug Metabolism and Personalized Therapy. 2019:34(2).
- Patel MM, Patel RJ. Linagliptin loaded Solid-SMEEDS for enhanced solubility and dissolution: Formulation development and optimization by D-optimal design. Journal of Drug Delivery and Therapeutics. 2019;9(2):47-56.
- Veni DK, Gupta NV. Development and evaluation of Eudragit coated environmental sensitive solid lipid nanoparticles using central composite design module for enhancement of oral bioavailability of linagliptin. International Journal of Polymeric Materials and Polymeric Biomaterials. 2019;69(7):407-418.
- Putchakayala NSD, Morusu K, Ramisetty S, Ravoru N. Nanostructured Lipid Carriers: A Novel Platform in the Formulation of Targeted Drug Delivery Systems. Current Nanomedicine. 2025;15(1):26-49.
- Ghani SF, Ali Z, Shah KU, Mirza R, Alamri AH, Fatease AA, et al. Unveiling the potential of nano-structured lipid carriers for oral administration of cefepime: Bioavailability and safety investigations. Colloids Surf Physicochem Eng Aspects. 2025;718:136938.
- Sinhmar GK, Shah NN, Chokshi NV, Khatri HN, Patel MM. Process, optimization, and characterization of budesonideloaded nanostructured lipid carriers for the treatment of inflammatory bowel disease. Drug Development and Industrial Pharmacy. 2018;44(7):1078-1089.
- Motawea A, Borg T, Abd El-Gawad AE-GH. Topical phenytoin nanostructured lipid carriers: design and development. Drug Development and Industrial Pharmacy. 2017;44(1):144-157.
- 13. Baek J-S, Pham CV, Myung C-S, Cho C-W. Tadalafil-loaded nanostructured lipid carriers using permeation enhancers. Int J Pharm. 2015;495(2):701-709.
- 14. Varshosaz J, Ghaffari S, Khoshayand MR, Atyabi F, Dehkordi AJ, Kobarfard F. Optimization of freeze-drying condition of amikacin solid lipid nanoparticles using D-optimal

- experimental design. Pharmaceutical Development and Technology. 2010;17(2):187-194.
- Rahman H, Rasedee A, How CW, Abdul AB, Allaudin ZN, Othman Hh, et al. Zerumbone-loaded nanostructured lipid carriers: preparation, characterization, and antileukemic effect. International Journal of Nanomedicine. 2013:2769.
- 16. Ng WK, Saiful Yazan L, Yap LH, Wan Nor Hafiza WAG, How CW, Abdullah R. Thymoquinone-Loaded Nanostructured Lipid Carrier Exhibited Cytotoxicity towards Breast Cancer Cell Lines (MDA-MB-231 and MCF-7) and Cervical Cancer Cell Lines (HeLa and SiHa). BioMed Research International. 2015;2015:1-10.
- 17. Ghazy E, Abdulrasool AA, Al-Tamimi JJ, Ayash N. Nebivolol Hydrochloride Loaded Nanostructured Lipid Carriers as Transdermal Delivery System: Part 1: Preparation, Characterization and In Vitro Evaluation. Al Mustansiriyah Journal of Pharmaceutical Sciences. 2016;16(2):1-14.
- Gidwani B, Vyas A, Kaur CD. Cytotoxicity and pharmacokinetics study of nanostructured lipid carriers of mechlorethamine: Preparation, optimization and characterization. Particulate Science and Technology. 2019;38(1):23-33.
- Shah NV, Seth AK, Balaraman R, Aundhia CJ, Maheshwari RA, Parmar GR. Nanostructured lipid carriers for oral bioavailability enhancement of raloxifene: Design and in vivo study. Journal of Advanced Research. 2016;7(3):423-434
- Pal R, Mujahid M, Ahmad S. Formulation Development and in-vitro Evaluation of Linagliptin Transdermal Patch Using Permeability Enhancer. International Journal of Pharmaceutical Sciences Review and Research. 2023;82(1).
- Wu C, Ji P, Yu T, Liu Y, Jiang J, Xu J, et al. Naringenin-loaded solid lipid nanoparticles: preparation, controlled delivery, cellular uptake, and pulmonary pharmacokinetics. Drug Des Devel Ther. 2016:911.
- N. Abed H, A. Abdulrasool A, M. Ghareeb M. Controlled Release Floating Matrix Tablet of Captopril. Iraqi Journal of Pharmaceutical Sciences (P-ISSN 1683 - 3597 E-ISSN 2521 -3512). 2017;20(2):1-8.
- 23. Sharma D, Singh R, Singh G. Orally Disintegrating Tablets in Fixed Dose Combination containing Ambroxol Hydrochloride and Salbutamol Sulphate prepared by Direct Compression Technique: Formulation Design, Development and In-Vitro Evaluation. The Turkish Journal of Pharmaceutical Sciences. 2018.
- 24. Attari Z, Bhandari A, Jagadish PC, Lewis S. Enhanced ex vivo intestinal absorption of olmesartan medoxomil nanosuspension: Preparation by combinative technology. Saudi Pharmaceutical Journal. 2016;24(1):57-63.
- Anselmo CdS, Mendes TdC, Honorio TdS, do Carmo FA, Cabral LM, de Sousa VP. Development and validation of a dissolution test for lutein tablets and evaluation of intestinal permeability. Food Chem. 2016;210:63-69.
- 26. Abed HN, A. Hussein A. Ex-Vivo Absorption Study of a Novel Dabigatran Etexilate Loaded Nanostructured Lipid Carrier Using Non-Everted Intestinal Sac Model. Iraqi Journal of Pharmaceutical Sciences (P-ISSN: 1683 3597, E-ISSN: 2521 3512). 2019;28(2):37-45.
- Shishu, Maheshwari M. Comparative bioavailability of curcumin, turmeric and Biocurcumax[™] in traditional vehicles using non-everted rat intestinal sac model. J Funct Foods. 2010;2(1):60-65.
- 28. Bothiraja C, Pawar AP, Dama GY, Joshi PP, Shaikh

- KS. Novel solvent-free gelucire extract of Plumbago zeylanica using non-everted rat intestinal sac method for improved therapeutic efficacy of plumbagin. Journal of Pharmacological and Toxicological Methods. 2012;66(1):35-42
- Javed S, Mangla B, Almoshari Y, Sultan MH, Ahsan W. Nanostructured lipid carrier system: A compendium of their formulation development approaches, optimization strategies by quality by design, and recent applications in drug delivery. Nanotechnology Reviews. 2022;11(1):1744-1777.
- How CW, Rasedee A, Abbasalipourkabir R. Characterization and Cytotoxicity of Nanostructured Lipid Carriers Formulated With Olive Oil, Hydrogenated Palm Oil, and Polysorbate 80. IEEE Trans NanoBiosci. 2013;12(2):72-78.
- 31. Shah P, Chavda K, Vyas B, Patel S. Formulation development of linagliptin solid lipid nanoparticles for oral bioavailability enhancement: role of P-gp inhibition. Drug Delivery and Translational Research. 2020;11(3):1166-1185.
- Lee Y-C, Dalton C, Regler B, Harris D. Drug solubility in fatty acids as a formulation design approach for lipid-based formulations: a technical note. Drug Development and Industrial Pharmacy. 2018;44(9):1551-1556.
- Li H, Chen M, Su Z, Sun M, Ping Q. Size-exclusive effect of nanostructured lipid carriers on oral drug delivery. Int J Pharm. 2016;511(1):524-537.
- 34. Danaei M, Dehghankhold M, Ataei S, Hasanzadeh Davarani F, Javanmard R, Dokhani A, et al. Impact of Particle Size and Polydispersity Index on the Clinical Applications of Lipidic Nanocarrier Systems. Pharmaceutics. 2018;10(2):57.
- 35. Wulff-Pérez M, Torcello-Gómez A, Gálvez-Ruíz MJ, Martín-Rodríguez A. Stability of emulsions for parenteral feeding: Preparation and characterization of o/w nanoemulsions with natural oils and Pluronic f68 as surfactant. Food Hydrocolloids. 2009;23(4):1096-1102.
- 36. Laxmi M, Bhardwaj A, Mehta S, Mehta A. Development and characterization of nanoemulsion as carrier for the enhancement of bioavailability of artemether. Artificial Cells, Nanomedicine, and Biotechnology. 2014;43(5):334-344
- Liu D, Jiang S, Shen H, Qin S, Liu J, Zhang Q, et al. Diclofenac sodium-loaded solid lipid nanoparticles prepared by emulsion/solvent evaporation method. J Nanopart Res. 2010;13(6):2375-2386.
- Dai W, Zhang D, Duan C, Jia L, Wang Y, Feng F, et al. Preparation and characteristics of oridonin-loaded nanostructured lipid carriers as a controlled-release delivery system. Journal of Microencapsulation. 2010;27(3):234-241.
- Formulation and Evaluation of Microemulsion Based Topical Hydrogel Containing Lornoxicam. Journal of Applied Pharmaceutical Science. 2014.
- 40. Joshi M, Patravale V. Nanostructured lipid carrier (NLC) based gel of celecoxib. Int J Pharm. 2008;346(1-2):124-132.
- 41. Madan J, Dua K, Khude P. Development and evaluation of solid lipid nanoparticles of mometasone furoate for topical delivery. International Journal of Pharmaceutical Investigation. 2014;4(2):60.
- The Merck Index: An Encyclopedia of Chemicals, Drugs, and Biologicals (14th edition). Reference Reviews. 2007;21(6):40-40.
- 43. Patil GB, Patil ND, Deshmukh PK, Patil PO, Bari SB. Nanostructured lipid carriers as a potential vehicle for Carvedilol delivery: Application of factorial design approach.

- Artificial Cells, Nanomedicine, and Biotechnology. 2014;44(1):12-19.
- 44. Jia L-J, Zhang D-R, Li Z-Y, Feng F-F, Wang Y-C, Dai W-T, et al. Preparation and characterization of silybin-loaded nanostructured lipid carriers. Drug Deliv. 2009;17(1):11-18.
- 45. Nikolić S, Keck CM, Anselmi C, Müller RH. Skin photoprotection improvement: Synergistic interaction between lipid nanoparticles and organic UV filters. Int J Pharm. 2011;414(1-2):276-284.
- 46. Sangsen Y, Laochai P, Chotsathidchai P, Wiwattanapatapee R. Effect of Solid Lipid and Liquid Oil Ratios on Properties of Nanostructured Lipid Carriers for Oral Curcumin Delivery. Advanced Materials Research. 2014;1060:62-65.
- Reis S, Neves, Lúcio, Martins, Lima. Novel resveratrol nanodelivery systems based on lipid nanoparticles to enhance its oral bioavailability. International Journal of Nanomedicine. 2013:177.
- 48. Kedar U, Phutane P, Shidhaye S, Kadam V. Advances in polymeric micelles for drug delivery and tumor targeting. Nanomed Nanotechnol Biol Med. 2010;6(6):714-729.
- 49. Das S, Ng WK, Tan RBH. Are nanostructured lipid carriers (NLCs) better than solid lipid nanoparticles (SLNs): Development, characterizations and comparative evaluations of clotrimazole-loaded SLNs and NLCs? Eur J Pharm Sci. 2012;47(1):139-151.
- Venkateswarlu V, Manjunath K. Preparation, characterization and in vitro release kinetics of clozapine solid lipid nanoparticles. Journal of Controlled Release. 2004;95(3):627-638.
- Thomas Barden A, De Abreu Engel RE, Chagas Campanharo S, Volpato NM, Scherman Schapoval EE. Characterization of Linagliptin Using Analytical Techniques. Drug Analytical Research. 2017;1(2):30-37.
- 52. Gaur PK, Mishra S, Bajpai M, Mishra A. Enhanced Oral Bioavailability of Efavirenz by Solid Lipid Nanoparticles:In Vitro Drug Release and Pharmacokinetics Studies. BioMed Research International. 2014;2014:1-9.
- 53. Jain K, Sood S, Gowthamarajan K. Optimization of

- artemether-loaded NLC for intranasal delivery using central composite design. Drug Deliv. 2014;22(7):940-954.
- 54. Kovacevic A, Savic S, Vuleta G, Müller RH, Keck CM. Polyhydroxy surfactants for the formulation of lipid nanoparticles (SLN and NLC): Effects on size, physical stability and particle matrix structure. Int J Pharm. 2011;406(1-2):163-172.
- 55. Felton LA. A Review of: "Handbook of Pharmaceutical Excipients, 5th edition". Drug Development and Industrial Pharmacy. 2006;32(8):1003-1003.
- 56. Hu F-Q, Jiang S-P, Du Y-Z, Yuan H, Ye Y-Q, Zeng S. Preparation and characteristics of monostearin nanostructured lipid carriers. Int J Pharm. 2006;314(1):83-89.
- 57. Bashah NAA, Awel E, Amri N, Alrozi R, Yaakob N, Zubir NA, et al. Role of temperature on colloidal behavior of gold nanoparticles dispersed in organic and aqueous media. AIP Conference Proceedings: Author(s); 2017. p. 020281.
- 58. Alshamsan A, Kazi M, Badran MM, Alanazi FK. Role of Alternative Lipid Excipients in the Design of Self-Nanoemulsifying Formulations for Fenofibrate: Characterization, in vitro Dispersion, Digestion and ex vivo Gut Permeation Studies. Front Pharmacol. 2018;9.
- Mishra A, Imam SS, Aqil M, Ahad A, Sultana Y, Ameeduzzafar, et al. Carvedilol nano lipid carriers: formulation, characterization and in-vivo evaluation. Drug Deliv. 2016;23(4):1486-1494.
- 60. Gamal W, Fahmy RH, Mohamed MI. Development of novel amisulpride-loaded liquid self-nanoemulsifying drug delivery systems via dual tackling of its solubility and intestinal permeability. Drug Development and Industrial Pharmacy. 2017;43(9):1530-1538.
- Garg A, Bhalala K, Tomar DS, Wahajuddin. In-situ single pass intestinal permeability and pharmacokinetic study of developed Lumefantrine loaded solid lipid nanoparticles. Int J Pharm. 2017;516(1-2):120-130.
- Mendes M, Soares HT, Arnaut LG, Sousa JJ, Pais AACC, Vitorino C. Can lipid nanoparticles improve intestinal absorption? Int J Pharm. 2016;515(1-2):69-83.

